Green Chemistry

Accepted Manuscript

This article can be cited before page numbers have been issued, to do this please use: Y. Fan, S. Li, J. Bao, L. Shi, Y. Yang, F. Yu, P. Gao, H. Wang, L. Zhong and Y. Sun, *Green Chem.*, 2018, DOI: 10.1039/C8GC00971F.

ROYAL SOCIETY OF CHEMISTRY

rsc.li/green-chem

View Article Online
DOI: 10.1039/C8GC00971F

Hydrofunctionalization of olefins to value-added chemicals via photocatalytic coupling[†]

Yonghui Fan,[a,b] Shenggang Li,[a,c] Jingxian Bao,[a,b] Lei Shi, [a,b] Yanzhang Yang,[a,d] Fei Yu,[a,d] Peng Gao,[a] Hui Wang,[a] Liangshu Zhong,*[,a,c] and Yuhan Sun*[,a,c]

[a] Key Laboratory of Low-Carbon Conversion Science and Engineering, Shanghai Advanced Research Institute, Chinese Academy of Sciences, Shanghai 201203, China

[b] Department of Chemistry, College of Sciences, Shanghai University, Shanghai 200444, China

[c] School of physical Science and Technology, ShanghaiTech University, Shanghai 201210, China

[d] University of the Chinese Academy of Sciences, Beijing 100049, China

* E-mail: zhongls@sari.ac.cn; sunyh@sari.ac.cn

[†] Electronic Supplementary Information (ESI) available. See DOI:10.1039/x0xx00000x

A green strategy was developed for synthesis of various value-added chemicals using methanol, acetonitrile, acetic acid, acetone and ethyl acetate as the hydrogen source by coupling them with olefins over heterogeneous photocatalysts. A radical coupling mechanism was proposed for the hydrofunctionalization of olefins with methanol to higher aliphatic alcohols over the Pt/TiO_2 catalyst as the model reaction. C-H bond cleavage and C-C bond formation between photogenerated radicals and terminal olefins were accomplished in a single reaction at high efficiency. Our approach is atomically economical with high anti-Markovnikov regioselectivity and promising application potential under mild reaction conditions.

Olefins are commonly used as the feedstock for the production of various value-added chemicals including alcohols, acids, esters and nitriles via hydrofunctionalization in industry[1-3]. For example, the conventional synthesis method for higher aliphatic alcohols is through the hydrogenation of aldehydes, whereas aldehydes are produced via homogeneous hydroformylation of terminal olefins with syngas under high pressure (Scheme 1a) [4-8]. The oxidation of aldehydes yields aliphatic acids, which can be further converted into esters via esterification. Although significant progress has been made in catalyst development for the hydroformylation reaction[9], expensive Rh-based homogeneous catalysts are still usually required. In addition, both limited product selectivity and difficulty in catalyst recovery make the process less economically viable and environmentally friendly. Yang's group[10, 11] reported a CeO_2−Pt@mSiO_2 heterogeneous catalyst to convert methanol and ethylene into propanal via tandem hydroformylation, where methanol served as both the C1 feedstock and the hydrogen source to replace syngas with the additional benefit of facile catalyst recycle. However, it remains difficult to avoid by-products such as iso-aldehydes and alkanes, limiting the yield of the n-aldehydes target product. As for another value-added olefin-derived chemicals, nitriles are widely used in industry[12]. The present industrial route for the anti-Markovnikov hydrocyanation of olefins to nitriles is the DuPont adiponitrile process using nickel triarylphosphite catalyst[13]. However, such a route is impractical for routine chemical synthesis for the severe safety concern of HCN, which is extremely toxic and explosive (Scheme 1b). To avoid using HCN, Fang *et al.*[14] reported a nickel-catalyzed transfer hydrocyanation reaction between alkyl nitriles and olefins. However, other olefins were also generated as by-products in this process. Obviously, it is highly desirable yet challenging to develop a single-step olefin hydrofunctionalization process for synthesizing value-added chemicals with an inexpensive and safe hydrofunctionalization source under mild reaction conditions.

The realization of C-H bond cleavage and C-C or C-N bond formation through photocatalytic coupling has been extensively studied in organic synthesis over the last decade[15-20]. Recently, Wu *et al.*[15] reported that aromatic photocatalytic benzene amination and hydroxylation over cobalt-catalyst under unusually mild conditions in excellent yields and selectivities. And Li *et al.*[17] built new C-C bond by photo-induced methylation of heteroarenes with MeOH as both the solvent and the methylation source. In addition, numerous photo-catalyzed homogeneous systems have been developed to realize the functionalization of olefins[21-23]. Compared with conventional thermal reactions, photochemical reactions occur under unparalleled mild conditions[24] and, in many case, have a high product selectivity[25, 26]. In recently years, radical hydroxyalkylation of olefins with alcohol or nitrile have also been reported [27, 28]. However, the focus on the approach of synthesis value-added chemicals via heterogeneous photocatalysis from olefins and cheap, readily available, and abundant small molecules is yet not enough.

View Article Online
DOI: 10.1039/C8GC00971F

In order to develop a green and atomic economic olefin hydrofunctionalization process for synthesizing value-added chemicals, herein, a route for synthesizing various fine chemicals including alcohols, acids, esters, ketones and nitriles from olefins was developed by hydrofunctionalization with high atomic economy and anti-Markovnikov regioselectivity via heterogeneous photocatalytic coupling (Scheme 1c). C-H bond cleavage and C-C bond formation between photogenerated radicals and terminal olefins were accomplished in a single reaction at high efficiency. Our catalytic strategy is simple and effective with high atomic economy and promising application potential.

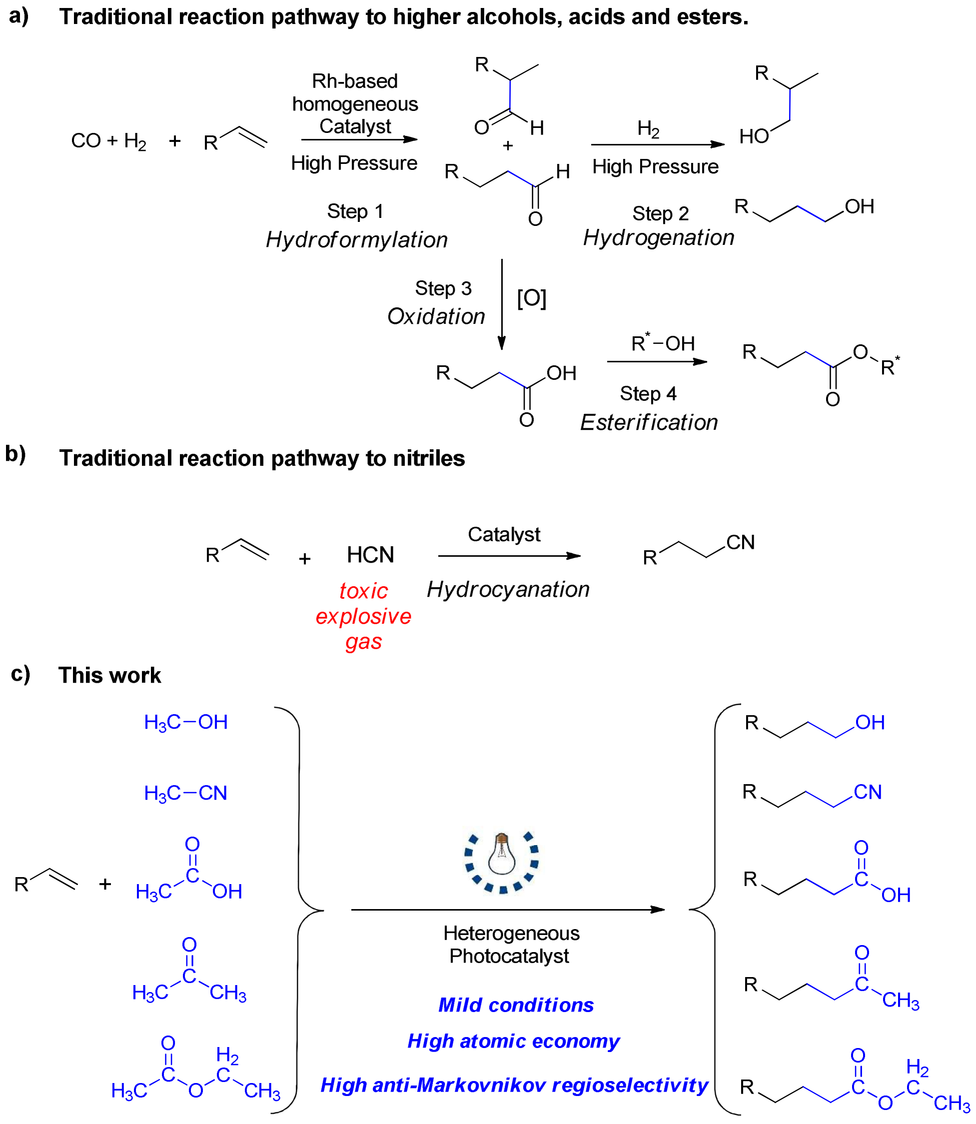

Scheme 1. Development of the protocol for hydrofunctionalization of olefins and our strategy for hydrofunctionalization of olefins via photocatalytic coupling.

View Article Online
DOI: 10.1039/C8GC00971F

Table 1. Hydrofunctionalization of olefins with methanol, acetonitrile, acetic acid, acetone or ethyl acetate.

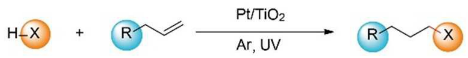

X= $-CH_2OH$; $-CH_2CN$; $-CH_2COOH$; $-CH_2COOC_2H_5$; $-CH_2COCH_3$

Entry[a]	Substrate	Olefins	Target product	TON ×10^3	TOF (h^{-1})×10^3	Selectivity to target product (%)	Anti-Markovnikov regioselectivity (%)
1				18.0	1.2	87.2	90
2		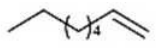	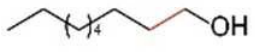	33.1	2.2	84.0	92
3		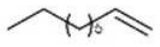	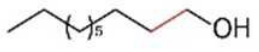	34.6	2.3	74.6	93
4		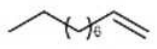	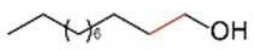	45.3	3.0	62.3	93
5			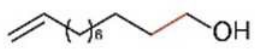	14.9	1.0	54.4	100
6		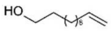	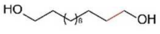	59.2	3.9	57.7	100
7		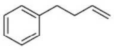	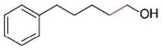	105.2	7.0	77.0	100
8		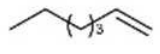	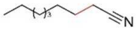	44.3	3.0	100.0	100
9				55.9	3.7	100.0	100
10				56.7	3.8	100.0	100
11		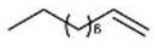	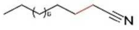	77.0	5.1	100.0	100
12	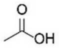	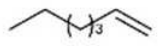	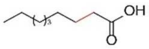	437.8	21.9	91.4	100
13			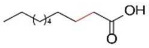	585.0	39.0	79.2	100
14			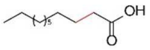	711.8	47.5	82.0	100
15				782.7	52.2	74.6	100
16		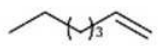	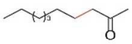	684.9	45.7	76.1	100
17	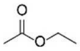		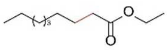	223.8	14.9	31.8	100

[a] Reaction condition: 1 mmol of olefin substrates，50 mg of photocatalyst in 50 mL of methanol, acetonitrile, acetic acid, acetone, ethyl acetate, respectively. The reaction were conducted under argon atmosphere at 60 °C (Entry 1-7) or 50 °C (Entry 8-17) under Xe lamp irradiation (200-400 nm) with light intensity of 100 mW/cm^2. The reaction time was 15 h. TON and TOF were calculated based on the target product.

DOI: 10.1039/C8GC00971F

Pt/TiO_2 was used as the model photocatalyst (Figure S1) for the hydrofunctionalization of olefins via photocatalytic coupling with methanol, acetonitrile, acetic acid, acetone and ethyl acetate. Various value-added chemicals including long-chain alcohols, nitriles, carboxylic acids, ketones, and esters were produced in one-step with high selectivity (Table 1). For the coupling of methanol and olefins to yield higher aliphatic alcohols, the anti-Markovnikov regioselectivity was up to 90% (Entry 1-7), and the main byproducts were acetal and alkane (Figure S2). Acetonitrile is an excellent substrate for producing nitriles, and our synthetic route not only avoids the use of the lethal HCN but also achieves nearly perfect chemoselectivity and regioselectivity (Entry 8-11). In addition, acetic acid (Entry 12-15), acetone (Entry 16) and ethyl acetate (Entry 17) can also be utilized to generate the desired products with very high anti-Markovnikov regioselectivity and atomic economy. Meanwhile, a broad range of olefins with different carbon chain lengths were examined and showed excellent catalytic performance. And the catalytic activity based on TON and TOF showed to be improved with the increase in the carbon number of olefin. Besides, substituted olefins such as 1,9-decadiene, 10-undecen-1-ol, 4-phenyl-1-butene were also successfully converted into the desired higher aliphatic alcohols with 100% regioselectivity (Entry 5-7).

To further investigate the factors affecting the photocatalytic performance, coupling between 1-decene and methanol was chosen as the model reaction. The control experiment clearly indicated that the desired reaction required both light and the photocatalyst, because no desired reaction occurred without either light or the photocatalyst. Under typical conditions, only trace amount of higher aliphatic alcohol ($C_{11}H_{23}OH$) was obtained at much lower TON of 10.3×10^{-3} for the sole TiO_2 catalyst. Increasing TON and TOF with the addition of Pt nanoparticles was attributed to the reduced probability for the recombination of photogenerated electrons and holes due to the transfer of the photoelectrons to Pt[29] (Table 2, Entries 3-6). However, the TON and TOF decreased with the further increasing the Pt loading as the higher loading of Pt enhanced the hydrogenation of olefin to alkane (Table 2, Entries 7 and 8). Other noble metals were explored (Table 2, Entries 9-11), which also significantly improved the catalytic activity. We also investigated the effect of reaction temperature on the

View Article Online
DOI: 10.1039/C8GC00971F

catalytic performance. The result showed that there was no product at 20℃. As shown in Figure S3, both the TON and the selectivity to higher aliphatic alcohol increased with the increase of reaction temperature. When certain amount of water was added to the reaction system, the selectivity of the higher aliphatic alcohol increased. This is likely due to the enhanced production of the •OH radical from water, which can activate methanol to form stable intermediates[17, 30-32] (Table S1), as discussed below. A wide range of alcohols were found to be effective as the hydrofunctionalization source for the coupling reaction and all the obtained higher aliphatic alcohols possessed perfect anti-Markovnikov regioselectivity (Table 3). In addition, with the sequence of ethanol, propanol and isopropanol, the TON and TOF of the desired product increased markedly, suggesting the trend in the catalytic activity to coincide with the stability of the α-C free radical intermediates (tertiary > secondary > primary)[33]

Table 2. Catalytic performance of controlled experiment for synthesis higher aliphatic alcohol via photocatalysis[a]

Entry	Catalyst	Noble metal loading (wt%)	TON $\times 10^3$	TOF (h^{-1}) $\times 10^3$	Selectivity to higher aliphatic alcohol (%)	Anti-Markovnikov regioselectivity (%)
1[b]	-	-	-	-	-	-
2[c]	Pt/TiO_2	0.44	-	-	-	-
3	TiO_2	-	10.3	0.7	85.3	94
4	Pt/TiO_2	0.14	23.9	1.6	42.6	95
5	Pt/TiO_2	0.29	24.2	1.6	43.3	95
6	Pt/TiO_2	0.44	45.3	3.0	62.3	93
7	Pt/TiO_2	0.70	22.5	1.5	64.2	94
8	Pt/TiO_2	1.22	0	0	0	-
9	Pd/TiO_2	0.48	89.7	6.0	36.3	85
10	Ru/TiO_2	0.48	94.9	6.3	52.5	90
11	Au/TiO_2	0.48	31.9	2.1	42.8	85

[a] Reaction condition: 1 mmol of 1-decene，50 mg of photocatalyst in 50 mL of methanol. The reaction were conducted under argon atomsphere at 60 °C under Xe lamp irradiation (200-400 nm) with light intensity of 100 mW/cm^2. The reaction time was 15 h. TON and TOF were calculated based on the target product. [b] Entry 1: no photocatalyst under illumination. [c] Entry 2: at dark condition

View Article Online
DOI: 10.1039/C8GC00971F

Table 3. Investigation of the scope of alcohol substrates.

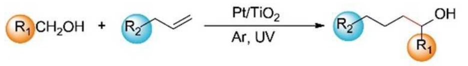

Entry*	Substrate	Target product	TON × 10^3	TOF (h^{-1}) × 10^3	Selectivity to target product (%)	A/(P+A)	Anti-Markovnikov regioselectivity (%)
1			45.3	3.0	62.3	0.92	93
2	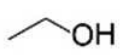	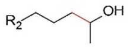	83.2	5.6	86.8	0.97	100
3	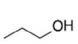	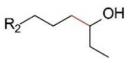	207.9	13.9	79.1	0.93	100
4	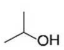	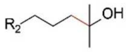	282.6	28.3	79.7	0.86	100

∗ The reaction time was 15 h (Entry 1-3) or 10 h (Entry 4). TON and TOF were calculated based on the target product.

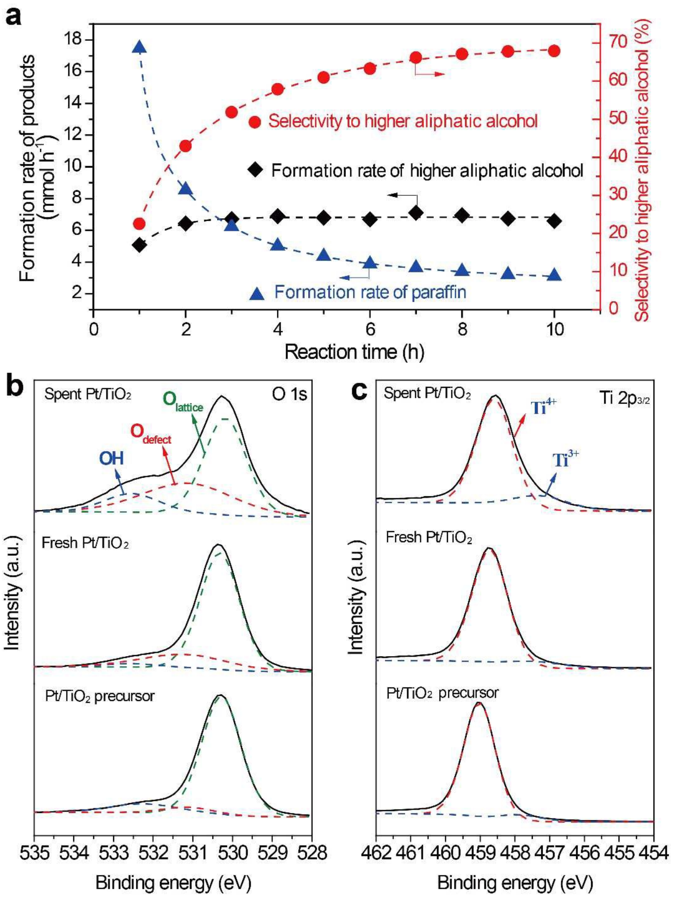

View Article Online
DOI: 10.1039/C8GC00971F

Fig. 1. Photocatalytic performance with time-on-stream and X-ray photoelectron spectra of Pt/TiO_2 at different stages. **a,** Formation rates of higher aliphatic alcohol and alkane and selectivity to higher aliphatic alcohols with time-on-stream. **b,** O 1s XPS spectrum of Pt/TiO_2 catalysts. XPS O1s spectra for the sample can be de-convoluted into three distinct peaks: the main oxide peak at 530.3 eV (‘$O_{lattice}$’) and two additional peaks at 531.2 eV and 532.5 eV, which were assigned to O atoms next to defects (‘O_{defect}’) and surface hydroxyls (‘OH’), respectively. **c,** Ti $2p_{3/2}$ XPS spectrum of Pt/TiO_2 catalysts. XPS Ti $2p_{3/2}$ spectra for the sample can be de-convoluted into two distinct peaks: the Ti^{4+} peak at 459.0 eV and Ti^{3+} peak at 457.9 eV, respectively.

We further examined the photocatalytic performance with time-on-stream. The formation rate of higher aliphatic alcohol increased first and then stabilized with time-on-stream while the production rate of alkane declined rapidly. Additionally, the selectivity to higher aliphatic alcohols increased quickly with time-on-stream especially during the first three hours (Fig. 1a). It suggested that defects on the photocatalyst surface generated by UV irradiation promoted the coupling[34]. The Ti^{3+} surface defect was previously proposed as one of the most important surface species, playing an essential role in the photocatalytic process[35]. Indeed, the photogenerated electrons and holes were produced by UV radiation in Pt/TiO_2 and some of the photogenerated electrons were trapped, which reduced the Ti^{4+} cations into the Ti^{3+} state[36]. Based on the XPS experiments (Figure 1b, 1c), the relative amount of Ti^{3+} and O_{defect} increased after the reaction (Table S3), which may benefit the separation of electrons and holes and the formation of higher aliphatic alcohols.

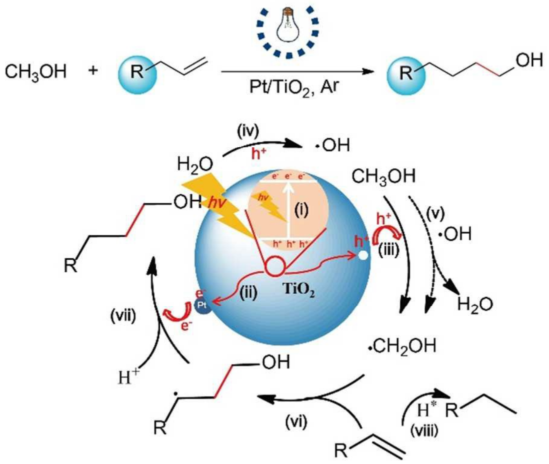

Fig. 2. Proposed photocatalytic mechanism for the photocatalytic coupling reaction between methanol and olefins. (i), Electron and hole pairs were generated by photoexcitation of the electrons from the valence band into the conduction band. (ii), The photogenerated electrons were

View Article Online
DOI: 10.1039/C8GC00971F

transferred to the Pt nanoparticles. (iii), The hole direct oxidized the absorbed alcohols into the corresponding α-C free hydroxyalkyl radicals. (iv) and (v), The holes oxidized H_2O to yield ·OH and ·OH radicals abstracted the H from α-C of the absorbed alcohols to form hydroxyalkyl radicals. (vi), Terminal olefins coupled with the hydroxyalkyl radicals to form a new C-C bond in the more stable secondary carbon-centred radicals. (vii), The carbon-centred radicals combined with electron and H^+ to form higher aliphatic alcohols. (viii), Terminal olefins were hydrogenated into alkanes as by-products.

Based on the above results, we proposed the following mechanism as shown in Fig. 2 for the photocatalytic coupling reaction between methanol and olefins over Pt/TiO_2. Under UV illumination, electrons were excited from the valence band to the conduction band of TiO_2, leading to the production of photogenerated electron and hole pairs (Step i). Next, the electron would transfer to Pt (Step ii) while the hole direct oxidized the absorbed alcohols into the corresponding α-C free hydroxyalkyl radicals. Meanwhile, the absorbed alcohols was also indirect oxidized by photogenerated ·OH radicals produced by oxidation of surface −OH groups or adsorbed water by the photogenerated holes (Step iv&v) [29,37]. *In situ* electron paramagnetic resonance (EPR) studies were performed to probe the intermediate radical species and DMPO-CH_2OH spin adduct was detected under illumination (Fig. S4)[32]. Upon the formation of the $\cdot CH_2OH$ radical, it was trapped immediately by the terminal carbon of olefins to generate a relatively stable carbon-centred radical intermediate (Step vi). This step was suggested to be the rate-limiting step during the alcohol/olefin coupling reaction. As secondary carbon-centred radicals were more stable than primary carbon-centred radicals for synthesis of higher aliphatic alcohol[38], the former were formed and further been reduced to alkyl anion, which protonated by H^+ to give the desired product with high anti-Markovnikov regioselectivity (Step vii). Furthermore, we also carried out first principles calculations using molecular density functional theory to further couple radical intermediates with terminal olefin (1-heptene as an example). The formation of secondary carbon-centred radical intermediates is thermodynamically favorable to that of primary carbon-centred radicals (Fig. 3). The coupling reaction is also exothermic due to stabilization of the carbon-centred radical, and should also have a relatively low energy barrier. Upon further reaction of the secondary radical intermediates with surface-adsorbed H*, anti-Markovnikov products are formed. In addition, there was a competitive pathway

View Article Online
DOI: 10.1039/C8GC00971F

for direct hydrogenation of the olefin to form alkane by absorbed H* (Step viii). Similar mechanisms were also proposed for the coupling reactions between other substrates and olefins (Scheme S1).

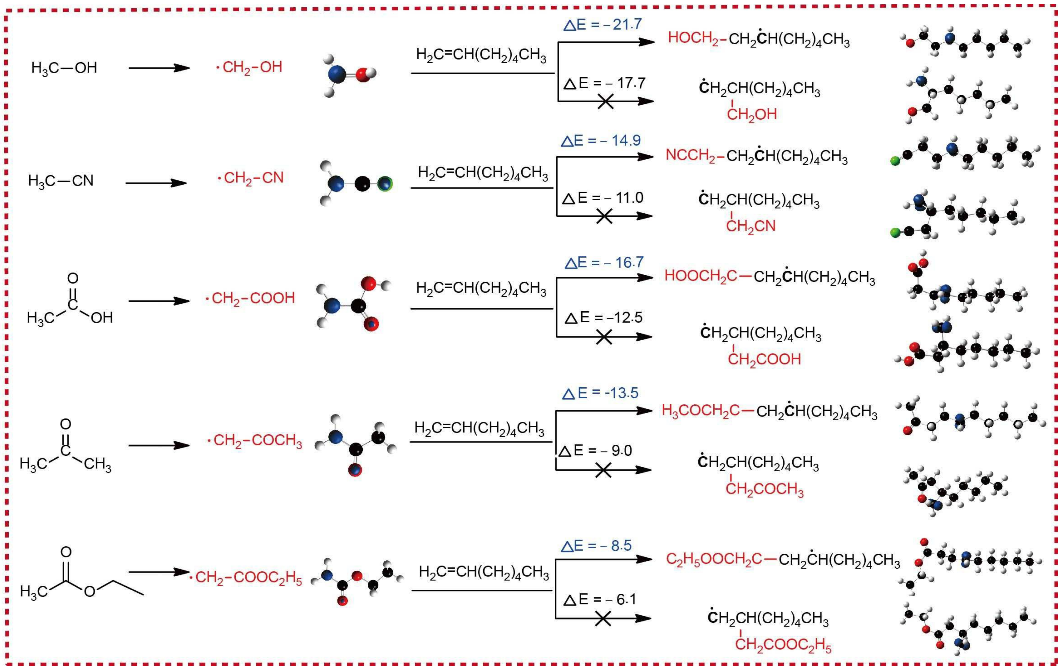

Fig. 3. First principles studies on the photocatalytic coupling reaction. The primary carbon-centered radicals which were formed by abstracting a H from the α-C of methanol, acetonitrile, acetic acid, acetone, and ethyl acetate are coupled with terminal olefin (1-heptene) to form secondary or primary carbon-centered radicals with energies shown in blue and black, respectively. Upon further hydrogenation, anti-Markovnikov and Markovnikov products are produced, and the latter are unfavorable. Energies at 0 K are given in kcal/mol. Spin density for the radicals is shown to illustrate the nature of the radical. Colors of the atoms: blue for Ti, red for O, black for C, green for N, and white for H.

For the photocatalytic hydrofunctionalization of olefins, the light absorption wavelength of the photocatalyst can be tuned through band gap engineering by doping TiO_2 with metal cations and anions, surface sensitization of TiO_2 with visible light absorbing dyes, molecular complexes, quantum dots, etc[29]. And visible-light-driven photocatalysts are under development for this approach. In addition, suitable junction structures should also lead to enhanced catalytic activity by improving the separation efficiency of photogenerated electrons and holes[39].

Conclusions

View Article Online
DOI: 10.1039/C8GC00971F

In summary, photocatalytic hydrofunctionalization of olefins provides a green and atom-efficient strategy for the synthesis of a great range of value-added chemicals all with nearly 100% anti-Markovnikov regioselectivity. Excellent performance was observed in the photocatalytic coupling reaction of olefins with methanol, acetonitrile, acetic acid, acetone and ethyl acetate. Experimental and computational studies were also performed to investigate the possible photocatalytic mechanism, which involved α-C-H cleavage and C-C bond formation via the coupling of photogenerated radical intermediates and terminal olefins. Our green strategy provides a promising route for synthesizing various fine chemicals by the photocatalytic coupling of olefins, and can be expected to have a broad impact in the field of chemical synthesis.

Conflicts of interest

There are no conflicts to declare.

Acknowledgement

This work has been supported by the National Key R&D Program of China (2017YFB0602202), the Natural Science Foundation of China (21573271, 91545112), and the Chinese Academy of Sciences (QYZDB-SSW-SLH035, XDA21020600).

Notes and references

1. K. A. Margrey and D. A. Nicewicz, *Acc. Chem. Res.*, 2016, **49**, 1997-2006.
2. J. R. Coombs and J. P. Morken, *Angew. Chem. Int. Ed.*, 2016, **55**, 2636-2649.
3. Z. Dong, Z. Ren, S. J. Thompson, Y. Xu and G. Dong, *Chem. Rev.*, 2017, **117**, 9333-9403.
4. D. Evans, J. A. Osborn, F. H. Jardine and G. Wilkinson, *Nature*, 1965, **208**, 1203-1204.
5. R. Franke, D. Selent and A. Borner, *Chem. Rev.*, 2012, **112**, 5675-5732.
6. J. Klosin and C. R. Landis, *Acc. Chem. Res.*, 2007, **40**, 1251-1259.
7. F. E. Paulik, *Catal. Rev.*, 1972, **6**, 49-84.
8. G. M. Torres, R. Frauenlob, R. Franke and A. Börner, *Catal. Sci. Technol.*, 2015, **5**, 34-54.
9. J. Pospech, I. Fleischer, R. Franke, S. Buchholz and M. Beller, *Angew. Chem. Int. Ed.*, 2013, **52**, 2852-2872.

View Article Online
DOI: 10.1039/C8GC00971F

10. Y. Yamada, C. K. Tsung, W. Huang, Z. Huo, S. E. Habas, T. Soejima, C. E. Aliaga, G. A. Somorjai and P. Yang, *Nat. Chem.*, 2011, **3**, 372-376.
11. J. Su, C. Xie, C. Chen, Y. Yu, G. Kennedy, G. A. Somorjai and P. Yang, *J. Am. Chem. Soc.*, 2016, **138**, 11568-11574.
12. M. Beller, J. Seayad, A. Tillack and H. Jiao, *Angew. Chem. Int. Ed.*, 2004, **43**, 3368-3398.
13. C. A. Tolrnan, *J. Chem. Edu.*, 1986, **63**, 199-201.
14. X. J. Fang, P. Yu and B. Morandi, *Science*, 2016, **351**, 832-836.
15. Y. W. Zheng, B. Chen, P. Ye, K. Feng, W. Wang, Q. Y. Meng, L. Z. Wu and C. H. Tung, *J. Am. Chem. Soc.*, 2016, **138**, 10080-10083.
16. Q. Xiao, S. Sarina, E. Jaatinen, J. Jia, D. P. Arnold, H. Liu and H. Zhu, *Green Chem.*, 2014, **16**, 4272.
17. W. Liu, X. Yang, Z.-Z. Zhou and C.-J. Li, *Chem*, 2017, **2**, 688-702.
18. H. Yuzawa, S. Yoneyama, A. Yamamoto, M. Aoki, K. Otake, H. Itoh and H. Yoshida, *Catal. Sci. Technol.*, 2013, **3**, 1739.
19. E. Wada, T. Takeuchi, Y. Fujimura, A. Tyagi, T. Kato and H. Yoshida, *Catal. Sci. Technol.*, 2017, **7**, 2457-2466.
20. Q. Yang, L. Zhang, C. Ye, S. Luo, L. Z. Wu and C. H. Tung, *Angew. Chem. Int. Ed.*, 2017, **56**, 3694-3698.
21. D. Ravelli, S. Protti and M. Fagnoni, *Acc Chem Res*, 2016, **49**, 2232-2242.
22. N. A. Romero and D. A. Nicewicz, *Chem Rev*, 2016, **116**, 10075-10166.
23. X. Z. Fan, J. W. Rong, H. L. Wu, Q. Zhou, H. P. Deng, J. D. Tan, C. W. Xue, L. Z. Wu, H. R. Tao and J. Wu, *Angew. Chem. Int. Ed.*, 2018, **57**,1-6.
24. M. Fagnoni, D. Dondi, D. Ravelli and A. Albini, *Chem. Rev.*, 2007, **107**, 2725-2756.
25. X. Hu, G. Zhang, F. Bu and A. Lei, *ACS Catal.*, 2017, **7**, 1432-1437.
26. H. M. Wang, Q. Q. Lu, C. W. Chiang, Y. Luo, J. F. Zhou, G. Y. Wang and A. W. Lei, *Angew. Chem. Int. Ed.*, 2017, **56**, 595-599.
27. Z. Li, Y. Xiao and Z. Q. Liu, *Chem Commun (Camb)*, 2015, **51**, 9969-9971.
28. Y. Tian and Z.-Q. Liu, *Green Chem.*, 2017, **19**, 5230-5235.
29. Y. Ma, X. Wang, Y. Jia, X. Chen, H. Han and C. Li, *Chem. Rev.*, 2014, **114**, 9987-10043.
30. H. Fischer, *Mol. Phys.*, 1965, **9**, 149-152.

31. H. Hussain, G. Tocci, T. Woolcot, X. Torrelles, C. L. Pang, D. S. Humphrey, C. M. Yim, D. C. Grinter, G. Cabailh, O. Bikondoa, R. Lindsay, J. Zegenhagen, A. Michaelides and G. Thornton, *Nat. Mater.*, 2017, **16**, 461-466.
32. H. Zhang, W. Zhang, M. Zhao, P. Yang and Z. Zhu, *Chem. Commun.*, 2017, **53**, 1518-1521.
33. J. Hioe, G. Savasci, H. Brand and H. Zipse, *Chem. Eur. J.*, 2011, **17**, 3781-3789.
34. W. Fang, M. Xing and J. Zhang, *J. Photoch. Photobio.*, 2017, **32**, 21-39.
35. L. B. Xiong, J. L. Li, B. Yang and Y. Yu, *J. Nanomater.*, 2012, DOI: 10.1155/2012/831524, 1-13.
36. G. Q. Lu, A. Linsebigler and J. T. Yates, *J. Phys. Chem.*, 1994, **98**, 11733-11738.
37. G. L. Chiarello, D. Ferri and E. Selli, *J. Catal.*, 2011, **280**, 168-177.
38. H. Kisch, *Angew. Chem. Int. Ed.*, 2013, **52**, 812-847.
39. J. Kou, C. Lu, J. Wang, Y. Chen, Z. Xu and R. S. Varma, *Chem. Rev.*, 2017, **117**, 1445-1514.

View Article Online
DOI: 10.1039/C8GC00971F

TOC

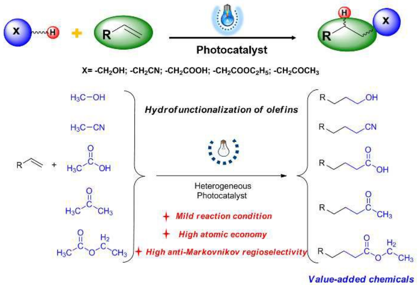

A sustainable strategy for hydrofunctionalization of olefins to value-added chemicals via photocatalytic cross-coupling was developed with high atomic economy.